Generation of propagating spin waves from regions of increased dynamic demagnetising field near magnetic antidots

C. S. Davies, A. V. Sadovnikov, S. V. Grishin, Yu. P. Sharaevskii, S. A. Nikitov, and V. V. Kruglyak

---

Articles you may be interested in

An antidot array as an edge for total non-reflection of spin waves in yttrium iron garnet films
Appl. Phys. Lett. **104**, 082412 (2014); 10.1063/1.4867026

Single antidot as a passive way to create caustic spin-wave beams in yttrium iron garnet films
Appl. Phys. Lett. **102**, 102409 (2013); 10.1063/1.4795293

Propagating volume and localized spin wave modes on a lattice of circular magnetic antidots
J. Appl. Phys. **103**, 07C507 (2008); 10.1063/1.2831792

Nonlinear transverse stabilization of spin-wave beams in magnetic stripes
Appl. Phys. Lett. **89**, 212501 (2006); 10.1063/1.2392821

Formation of envelope solitons from parametrically amplified and conjugated spin wave pulses
J. Appl. Phys. **93**, 8758 (2003); 10.1063/1.1558603

Generation of propagating spin waves from regions of increased dynamic demagnetising field near magnetic antidots

C. S. Davies,[1,a] A. V. Sadovnikov,[2,3] S. V. Grishin,[2] Yu. P. Sharaevskii,[2] S. A. Nikitov,[2,3] and V. V. Kruglyak[1]

[1]*School of Physics, University of Exeter, Stocker Road, Exeter EX4 4QL, United Kingdom*
[2]*Laboratory "Metamaterials," Saratov State University, Saratov 410012, Russia*
[3]*Kotel'nikov Institute of Radioengineering and Electronics, Russian Academy of Sciences, Moscow 125009, Russia*

We have used Brillouin Light Scattering and micromagnetic simulations to demonstrate a point-like source of spin waves created by the inherently nonuniform internal magnetic field in the vicinity of an isolated antidot formed in a continuous film of yttrium-iron-garnet. The field nonuniformity ensures that only well-defined regions near the antidot respond in resonance to a continuous excitation of the entire sample with a harmonic microwave field. The resonantly excited parts of the sample then served as reconfigurable sources of spin waves propagating (across the considered sample) in the form of caustic beams. Our findings are relevant to further development of magnonic circuits, in which point-like spin wave stimuli could be required, and as a building block for interpretation of spin wave behavior in magnonic crystals formed by antidot arrays. © 2015 AIP Publishing LLC. [http://dx.doi.org/10.1063/1.4933263]

The ability to excite propagating spin waves in magnetic media is of critical importance to the functionality and utility of any conceivable magnonic device. Generally, the character of waves excited in a medium depends on the nature and properties of the medium itself as well as the spatial and temporal character of the excitation. There are a wide variety of spin-wave stimuli available to researchers and engineers studying magnetization dynamics, ranging from the more conventional localized, fast varying magnetic fields[1–3] to focused optical pulses,[4,5] spin-transfer-torque oscillators,[6,7] grating couplers,[8,9] and resonant magnetic transducers,[10,11] for example. In particular, the latter mechanism can be traced back to that proposed by Schlömann in Ref. 12, who exploited the violation of the linear momentum conservation in media with broken translation invariance to enable coupling between long wavelength electromagnetic waves and short wavelength spin waves. This method is quite general since the translational invariance is broken by any magnetic nonuniformity, be that compositional nonuniformity or any other nonuniformity of the internal magnetic field.[13–15]

The magnetostatic spin waves[16] are well-known to have inherently anisotropic dispersion, which depends dramatically on the relative orientation of the magnetization M and the spin-wave wave vector k. Similarly to any other waves, the direction of propagation of spin waves in an anisotropic medium can be determined using so-called isofrequency curves, i.e., reciprocal space curves defining the combinations of wave vector components that satisfy the dispersion relation for a specific frequency. The direction of the spin-wave group velocity is given by the normal to the isofrequency curve. A remarkable feature of the isofrequency curves of magnetostatic spin waves is that large segments of

the curves are nearly straight.[17–19] If, therefore, spin waves with a broad range of wave vectors are excited, e.g., by a point-like source, the straight segments of the isofrequency curves lead to collinearity of the group velocities corresponding to wave vectors on those straight segments. In real space, this causes true spin-wave point-sources to emit tightly focused spin wave beams (commonly referred to as "spin-wave caustics")[20] with a two-fold symmetry. The practical realization of point-like spin-wave stimuli is non-trivial. Spin waves excited by a focused optical pulse[4] were observed to have the caustic character, but their frequency is difficult, if not impossible, to control. Spin-wave caustics have also been generated as a by-product of the collapse of non-linear spin-wave "bullets,"[21] via the diffraction of plane spin waves from narrow apertures[22–24] and antidots,[25] and via the excitation of localized edge modes.[26]

In this letter, we demonstrate excitation of propagating spin waves (and more specifically, spin-wave caustics) using magnetic non-uniformities created by patterning in magnetic films. Specifically, we pattern an isolated antidot within an otherwise continuous yttrium iron garnet (YIG) film. As a result of this, the distribution of the static and dynamic demagnetizing fields in the vicinity of the antidot is modified relative to the rest of the film. Then, we use a microstrip antenna with a width much greater than the antidot diameter to excite a high-frequency magnetic field that is approximately uniform in the vicinity of the antidot. The frequency of this harmonic field is tuned to selectively match the local resonance frequencies[27] of specific localized regions adjacent to the antidot. When the frequency exceeds that of the uniform ferromagnetic resonance (FMR) in the rest of the YIG film, the resonating regions do not support confined spin-wave modes but form instead localized point-like sources of spin waves propagating into the continuous film. We use Brillouin Light Scattering (BLS) microscopy to image

[a]Author to whom correspondence should be addressed. Electronic mail: csd203@exeter.ac.uk

© 2015 AIP Publishing LLC

and micromagnetic simulations to model the excited spin-wave caustic beams, verifying the functionality of the proposed mechanism of spin-wave excitation. The results presented here are applicable to the interpretation of the magnetization dynamics in magnonic antidot arrays (which have been extensively studied, e.g., in Refs. 28–46), while also elaborating the interpretation of the spin-wave scattering that was experimentally and theoretically studied in Ref. 25.

Fig. 1(a) presents a schematic of the investigated system. Specifically, we studied a $2 \times 8\,\text{mm}^2$ film of $10\,\mu\text{m}$ thick YIG epitaxially grown on a gadolinium gallium garnet (GGG) substrate. A single antidot of $100\,\mu\text{m}$ diameter was laser scribed in the center of the sample and positioned directly above the center of a $250\,\mu\text{m}$ wide microstrip antennae. The YIG/GGG bilayer was flipped so that its YIG side was directly facing the microstrip. This microstrip was loaded with microwave current pulses, of $500\,\text{ns}$ duration, $2\,\mu\text{s}$ repetition interval, and an average power of $1.25\,\text{dBm}$. The current produced microwave magnetic field h_mw that was approximately uniform in strength and distribution around the antidot. The entire system was uniformly magnetized by in-plane bias magnetic field $H_\text{B} = 500\,\text{Oe}$, which was applied parallel to the microstrip antenna.

Micromagnetic simulations of the observed magnetization dynamics were performed using the Object-Oriented Micro-Magnetic Framework (OOMMF).[47,48] The simulation parameters were chosen so as to model a YIG-like material, whereby the gyromagnetic ratio and magnetization of saturation were assumed to be $\gamma = 2.80\,\text{MHz/Oe}$ and $M_\text{S} = 140\,\text{G}$, respectively. The magneto-crystalline anisotropy and exchange energies were neglected. The mesh cell

size was $2 \times 2 \times 3.33\,\mu\text{m}^3$. The size of the whole simulated sample was $2000 \times 2000 \times 10\,\mu\text{m}^3$, and the antidot was modeled as a $10\,\mu\text{m}$ thick cylinder of $100\,\mu\text{m}$ diameter and zero magnetization. To suppress effects associated with the outer edges of the simulated sample, two-dimensional periodic boundary conditions[49] were implemented in its plane. In principle, this generated an array of widely spaced antidots. However, the spacing between antidots in the array was sufficiently greater than the antidot diameter, so that we could neglect the influence of inter-antidot coupling on the observed dynamics.

The static spatial distributions of the projections of the demagnetizing (H_dem) and total internal field ($H_\text{i} = H_\text{B} + H_\text{dem}$) onto the magnetization are shown in Figs. 1(b) and 1(c), respectively. The emergence of magnetic poles is clearly observed immediately above and below the antidot, where the demagnetizing field opposes the bias field. Expectedly, this leads to a local reduction of the internal field.[29] In contrast, the total internal field at the left and right sides of the antidot is actually increased, due to the demagnetizing field aligning with the bias field. This behavior of the demagnetizing field resembles the field of an isolated dipole and is therefore also anticipated. The regions of the reduced internal magnetic field can lead to confinement of spin-wave modes, as extensively discussed, e.g., in Refs. 29, 30, 32, and 35. In this letter, we instead focus on the possibility to excite propagating spin waves taking advantage of the regions of the increased internal magnetic field.

The uniform FMR frequency f_FMR of an in-plane magnetized continuous magnetic film is given by[50]

$$f_{FMR} = \gamma \sqrt{H_i(H_i + 4\pi M_S)}, \qquad (1)$$

where the internal magnetic field is actually equal to the bias magnetic field. The key axiom of finite-difference time-domain micromagnetic simulations[51] is that the internal field and magnetization orientation are both uniform in each cell of the mesh. Following the approach from Ref. 27, we can neglect the wave-vector dependent contributions to the effective magnetic field and calculate the distribution of the "local FMR frequency" (referred to as "local frequency" in the following) on a cell-by-cell basis, as shown in Fig. 2(a). The local frequency calculated in this way represents the FMR frequency of an infinite thin film experiencing the same internal magnetic field as in the specific cell. On the other hand, the physical meaning of the local frequency is the limiting value of the spin-wave frequency when $k \rightarrow 0$. This approximation (a more rigorous development of which is beyond the scope of this letter) allows us, e.g., to understand qualitatively the presence of quasi-uniform resonance modes confined above and below the antidot.[27,35] Moreover, as would be expected from Fig. 1(c), the regions left and right of the antidot reveal an increase in the local frequency, which then tends in a graded fashion[24] towards the FMR frequency of the continuous film (2.98 GHz). Obviously, these regions of increased local frequency are unable to confine spin waves. However, as one could infer from Refs. 11–15 and as we show in the following, they can be used to couple incident electromagnetic waves to propagating spin waves and thereby serve as localized magnonic sources.
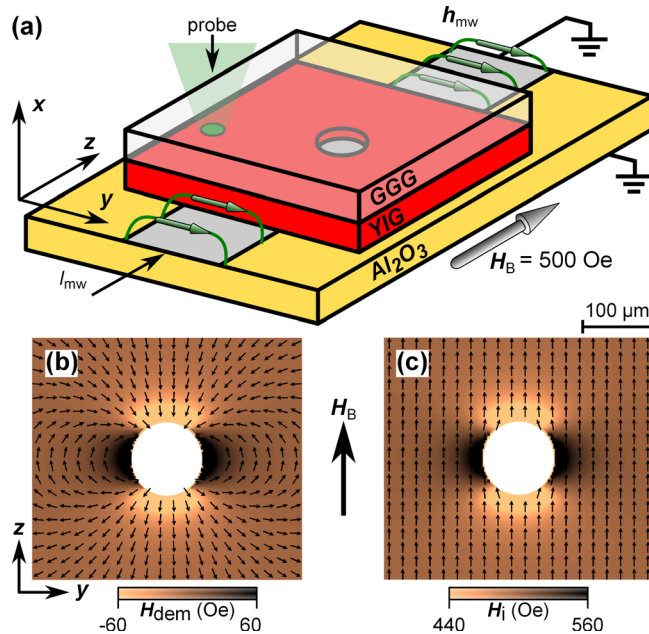

FIG. 1. (a) The studied sample is schematically shown. (b) The calculated distribution of the demagnetizing field is shown for the immediate vicinity of the antidot. The arrows show the local orientation of the demagnetizing field. The dark-bright scale represents the projection of the demagnetizing field onto the magnetization. (c) The calculated distribution of the total internal field is shown for the immediate vicinity of the antidot. The arrows show the local orientation of the magnetization (normalized and averaged over 10×10 cells). The dark-bright scale represents the projection of the internal field onto the magnetization.
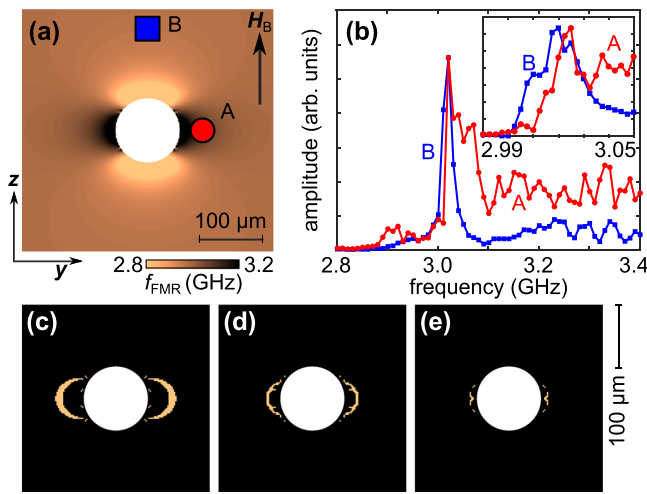
FIG. 2. (a) The distribution of the local frequency calculated according to Eq. (1) is shown for the immediate vicinity of the antidot. (b) The measured normalized BLS signals are shown for points A (immediately right of the antidot, red circles) and B (continuous film, blue squares) indicated in (a). The inset shows excitation signals acquired with higher frequency resolution. (c)–(e) Binary images (corresponding to that from panel (a)), where the bright regions have local frequencies approximately equal to 3.1 GHz, 3.2 GHz, and 3.3 GHz, respectively, are shown.
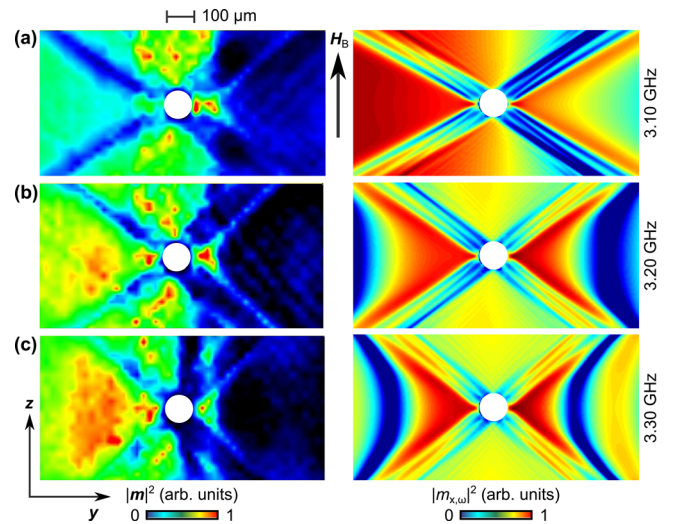

FIG. 3. Amplitude resolved BLS (left panels) and simulated BLS-like (right panels) images are shown for excitation frequencies of (a) 3.1 GHz, (b) 3.2 GHz, and (c) 3.3 GHz.

Our discussion so far has only been supported by the results and interpretation of static micromagnetic simulations. To verify our ideas experimentally, we used BLS microscopy[52] to image spin waves in the vicinity of the antidot. A laser beam of 532 nm wavelength was focused through the GGG substrate to a spot of 20 μm diameter on the YIG surface. The spectrum of coherently excited spin waves was recorded locally first from the continuous film and then immediately right of the antidot [Figs. 2(a) and 2(b)]. In the continuous film [point B in Fig. 2(a)], there is a sharp peak at 3.02 GHz with a full width at half-maximum (FWHM) of around 0.03 GHz, which corresponds approximately to the frequency of FMR of the continuous YIG film. In contrast, at point A located immediately right of the antidot, the maximum of the frequency spectra is shifted to 3.025 GHz. At frequencies above this, the BLS signal of lower strength is also clearly observed above this frequency, reflecting the graded variation of the local frequency distribution apparent from Fig. 2(a).

From the discussed nature of the demagnetizing field, it is evident that the regions of increased local frequency about and adjacent to the antidot should be distributed quasi-concentrically, as shown in Figs. 2(c)–2(e) where regions with local frequency of about 3.1, 3.2, and 3.3 GHz, respectively, are highlighted. Note the frequency interval used to generate these binary images is 100 MHz. A direct excitation of these half-ring shaped regions should lead to excitation of propagating spin waves via the Schlömann mechanism.[12] To verify this hypothesis, two-dimensional images of BLS signal in the vicinity of the antidot were recorded as a function of frequency. The measured maps of the dynamic magnetization distributions are presented on a logarithmic scale in the left panels of Figs. 3(a)–3(c). To corroborate the experimental observations, dynamic micromagnetic calculations were performed, in which the modeled sample now spanned a cuboid of $(8 \times 8 \times 0.01)$ mm^3 size discretized into

$(4 \times 4 \times 10)$ μm^3 mesh cells. A harmonic magnetic field with a spatial profile described by the Karlqvist equations[53] was used to mimic the Oersted field generated by the microstrip. Note that the large lateral width of the tessellated supercell was required to prevent spin waves from propagating across its boundaries. Indeed, typically, the Gilbert damping coefficient of YIG (1×10^{-4}) enables spin waves to propagate to centimeter distances. In the right panels of Figs. 3(a)–3(c), the power distribution of the Fourier-transformed dynamic out-of-plane component of the magnetization is shown, plotted so as to be comparable to the experimentally measured BLS images.

The results shown in Fig. 3 clearly and consistently demonstrate the excitation of spin waves forming caustic beams within the studied system. There are several features of note to be discussed. First, there is significant asymmetric excitation of plane magnetostatic surface spin waves (which are primarily observed on the left side of the antidot), as a result of the finite width of the microstrip and the non-reciprocal character of said spin waves.[16,54] Second, in addition to the caustic beams on the right side of the antidot, there are clear "extinction" lines on the left side. Third, the angle at which the spin wave caustics are emitted depends upon the frequency of excitation.[55] Last but not least, multiple spin wave caustic beams are observed in the micromagnetic simulations. These observations are consistent with those of Geniusz *et al.*[25] Here, using our earlier discussion of the nonuniformity of the internal field, we elaborate further on the physics underpinning the measurements reported in Ref. 25.

In Ref. 25, the authors were able to develop a reasonable interpretation of the data based on the picture of spin-wave scattering from the geometrical edges of the antidot, which is clearly not the case in the present case. Instead, the Schlömann mechanism is active here. Furthermore, one could argue that also in Ref. 25 the non-uniformities of the internal field [Fig. 1(c)] contributed to the scattering of the incident plane spin waves from the antidot. Indeed, when the plane spin waves of frequency f are incident upon a

region of magnetization with the same local frequency [Fig. 2(a)], the power of the plane wave can be resonantly transferred to the said region of magnetization.[56] The precessing magnetization in the region then serves as a source of secondary spin waves, which form the spin wave caustics observed in Ref. 25. In our case, the role of the plane spin waves is played by the incident microwave field. The multiple caustics observed both in Ref. 25 and in our Fig. 3 originate from the finite spatial extent of the excited resonances. This leads to the spin-wave caustic beams having a finite width (here, on the order of the antidot diameter). Due to the anisotropy of the spin-wave dispersion, the phase and group velocities are crudely orthogonal to each other. This leads to phase variation across the beam width, thereby creating an illusion of multiple caustic beams in the recorded images.

The left panels of Figs. 4(a)–4(c) present the dynamic out-of-plane component of the magnetization ($m_{x,a}$) for different values of the excitation frequency, i.e., the data from which the right panels of Figs. 3(a)–3(c) were derived. To illustrate the origin of the extinction lines, the background resulting from the plane spin waves excited due to the finite width of the waveguide was removed from the data. Specifically, we repeated the static and dynamic micromagnetic simulations for the same YIG sample with the antidot removed, i.e., for a continuous YIG film. The dynamic magnetization $m_{x,c}$ from the latter simulations was then used as the background, and the images presented in the right panels of Fig. 4(a)–4(c) were generated. Now, the spin wave caustics on both sides of the antidot are symmetrical in both amplitude and phase.[54] This calculation directly confirms the hypothesis of negative interference put forward in Ref. 25 to explain the origin of the extinction lines.

In conclusion, we have used the non-uniformity of the internal magnetic field inherent to patterned-film magnetic structures to realize a quasi-point-like source of spin waves. Using BLS imaging and micromagnetic simulations, we have deduced the magnetic ground state and associated distribution of local resonance frequency in the vicinity of a single antidot. Hence, upon exciting the entire sample by a microwave field at the frequency above that of the uniform FMR of the continuous film, we could selectively excite well-defined regions of the magnetization and thereby cause them to emit spin waves propagating in the form of caustic beams. Whilst the measurements here were performed on length scales of hundreds of micrometers, it is expected that the demonstrated mechanism of spin-wave excitation should be downscalable. The excited spin waves should form caustic beams as long as the anisotropy of the magnetostatic spin-wave dispersion persists. Furthermore, as the saturation magnetization increases, the demagnetizing fields also increase. Thus, the regions of increased local frequency should extend significantly further away from antidots patterned in such materials as permalloy or cobalt, while the range of excitable frequencies should extend further away from the FMR frequency of the continuous film. Our findings are relevant both to further development of magnonic technology, in which the implementation of point-like spin wave stimuli could be required, and as a building block—using which to understand and interpret the extensive studies of magnetization dynamics in magnonic crystals formed by antidot arrays.
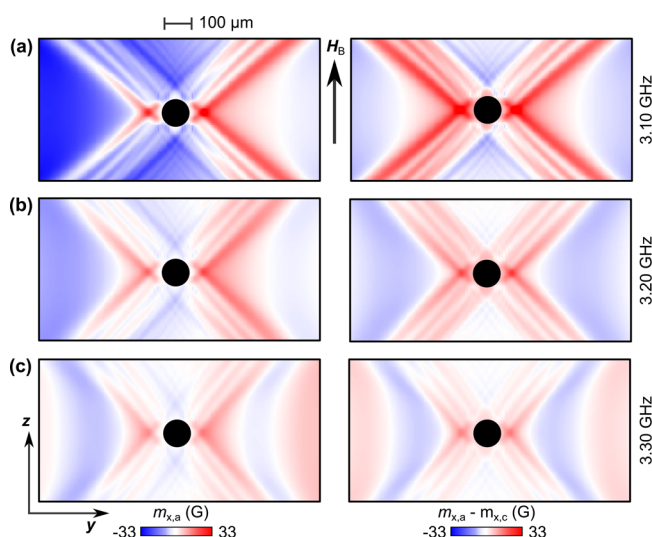
FIG. 4. The dynamic out-of-plane component of the magnetization of the YIG sample is shown for the excitation frequencies of (a) 3.10 GHz, (b) 3.20 GHz, and (c) 3.30 GHz. The left panels show the raw signal, while the right panels show the same signal with the background dynamics subtracted.

[1]W. K. Hiebert, A. Stankiewicz, and M. R. Freeman, "Direct observation of magnetic relaxation in a small permalloy disk by time-resolved scanning Kerr microscopy," Phys. Rev. Lett. **79**, 1134 (1997).

[2]A. V. Sadovnikov, C. S. Davies, S. V. Grishin, V. V. Kruglyak, D. V. Romanenko, Yu. P. Sharaevskii, and S. A. Nikitov, "Magnonic beam splitter: The building block of parallel magnonic circuitry," Appl. Phys. Lett. **106**, 192406 (2015).

[3]C. F. Adolff, M. Hänze, M. Pues, M. Weigand, and G. Meier, "Gyrational modes of benzenelike magnetic vortex molecules," Phys. Rev. B **92**, 024426 (2015).

[4]T. Satoh, Y. Terui, R. Moriya, B. A. Ivanov, K. Ando, E. Saitoh, T. Shimura, and K. Kuroda, "Directional control of spin-wave emission by spatially shaped light," Nat. Photonics **6**, 662 (2012).

[5]Y. Au, M. Dvornik, T. Davison, E. Ahmad, P. S. Keatley, A. Vansteenkiste, B. Van Waeyenberge, and V. V. Kruglyak, "Direct excitation of propagating spin waves by focused ultrashort optical pulses," Phys. Rev. Lett. **110**, 097201 (2013).

[6]V. E. Demidov, S. Urazhdin, and S. O. Demokritov, "Direct observation and mapping of spin waves emitted by spin-torque nano-oscillators," Nat. Mater. **9**, 984 (2010).

[7]M. Madami, S. Bonetti, G. Consolo, S. Tacchi, G. Carlotti, G. Gubbiotti, F. B. Mancoff, M. A. Yar, and J. Akerman, "Direct observation of a propagating spin wave induced by spin-transfer torque," Nat. Nanotechnol. **6**, 635 (2011).

[8]J. Sklenar, V. S. Bhat, C. C. Tsai, L. E. DeLong, and J. B. Ketterson, "Generating wave vector specific Damon-Eshbach spin waves in Py using a diffraction grating," Appl. Phys. Lett. **101**, 052404 (2012).

[9]H. Yu, G. Duerr, R. Huber, M. Bahr, T. Schwarze, F. Brandl, and D. Grundler, "Omnidirectional spin-wave nanograting coupler," Nat. Commun. **4**, 2702 (2013).

[10]Y. Au, T. Davison, E. Ahmad, P. S. Keatley, R. J. Hicken, and V. V. Kruglyak, "Excitation of propagating spin waves with global uniform microwave fields," Appl. Phys. Lett. **98**, 122506 (2011).

[11]Y. Au, E. Ahmad, O. Dmytriiev, M. Dvornik, T. Davison, and V. V. Kruglyak, "Resonant microwave-to-spin-wave transducer," Appl. Phys. Lett. **100**, 182404 (2012).

[12]E. Schlömann, "Generation of spin waves in nonuniform magnetic fields. I. Conversion of electromagnetic power into spinwave power and vice versa," J. Appl. Phys. **35**, 159 (1964).

[13]V. V. Tikhonov and A. V. Tolkachev, "Linear excitation of exchange spin-waves in implanted YIG-films," Fiz. Tverd. Tela **36**, 185 (1994).

[14]P. E. Zilberman, A. G. Temiryazev, and M. P. Tikhomirova, "Short-wavelength exchange dominated spin-waves and possible applications," Usp. Fiz. Nauk **165**, 1219 (1995).

[15]Y. I. Gorobets, A. N. Kuchko, and S. V. Vasil'yev, "Excitation of modulated spin waves by model one-dimension anisotropy defect," Fiz. Metall. Metalloved. **85**, 40 (1998) [Phys. Met. Metallogr. **85**, 272 (1998)].

[16]R. W. Damon and J. R. Eshbach, "Magnetostatic modes of a ferromagnet slab," J. Phys. Chem. Solids **19**, 308 (1961).

[17]A. V. Vashkovskii, A. V. Stalmakhov, and D. G. Shakhnazaryan, "Formation, reflection and refraction of wave-beams of magnetostatic waves," Izv. Vyssh. Uchebn. Zaved., Fiz. **31**, 67 (1988).

[18]A. V. Vashkovsky and E. H. Lock, "Properties of backward electromagnetic waves and negative reflection in ferrite films," Phys.-Usp. **49**, 389 (2006).

[19]E. H. Lock, "The properties of isofrequency dependences and the laws of geometrical optics," Phys.-Usp. **51**, 375 (2008).

[20]V. Veerakumar and R. E. Camley, "Magnon focusing in thin ferromagnetic films," Phys. Rev. B **74**, 214401 (2009).

[21]M. P. Kostylev, A. A. Serga, and B. Hillebrands, "Radiation of caustic beams from a collapsing bullet," Phys. Rev. Lett. **106**, 134101 (2011).

[22]V. E. Demidov, S. O. Demokritov, D. Birt, B. O'Gorman, M. Tsoi, and X. Li, "Radiation of spin waves from the open end of a microscopic magnetic-film waveguide," Phys. Rev. B. **80**, 014429 (2009).

[23]T. Schneider, A. A. Serga, A. V. Chumak, C. W. Sandweg, S. Trudel, S. Wolff, M. P. Kostylev, V. S. Tiberkevich, A. N. Slavin, and B. Hillebrands, "Nondiffractive subwavelength wave beams in a medium with externally controlled anisotropy," Phys. Rev. Lett. **104**, 197203 (2010).

[24]C. S. Davies, A. Francis, A. V. Sadovnikov, S. V. Chertopalov, M. T. Bryan, S. V. Grishin, D. A. Allwood, Yu. P. Sharaevskii, S. A. Nikitov, and V. V. Kruglyak, "Towards graded-index magnonics: Steering spin waves in magnonic networks," Phys. Rev. B **92**, 020408 (2015).

[25]R. Gieniusz, H. Ulrichs, V. D. Bessonov, U. Guzowska, A. I. Stognii, and A. Maziewski, "Single antidot as a passive way to create caustic spin-wave beams in yttrium iron garnet films," Appl. Phys. Lett. **102**, 102409 (2013).

[26]T. Sebastian, T. Brächer, P. Pirro, A. A. Serga, B. Hillebrands, T. Kubota, H. Naganuma, M. Oogane, and Y. Ando, "Nonlinear emission of spin-wave caustics from an edge mode of a microstructured $Co_2Mn_{0.6}Fe_{0.4}Si$ waveguide," Phys. Rev. Lett. **110**, 067201 (2013).

[27]A. N. Marchenko and V. N. Krivoruchko, "Magnetic structure and resonance properties of a hexagonal lattice of antidots," Low. Temp. Phys. **38**, 157 (2012).

[28]C. Yu, M. J. Pechan, W. A. Burgei, and G. J. Mankey, "Lateral standing spin waves in permalloy antidot arrays," J. Appl. Phys. **95**, 6648 (2004).

[29]O. N. Martyanov, V. F. Yudanov, R. N. Lee, S. A. Nepijko, H. J. Elmers, R. Hertel, C. M. Schneider, and G. Schönhense, "Ferromagnetic resonance study of thin film antidot arrays: Experiment and micromagnetic simulations," Phys. Rev. B **75**, 174429 (2007).

[30]S. Neusser, B. Botters, and D. Grundler, "Localization, confinement, and field-controlled propagation of spin waves in $Ni_{80}Fe_{20}$ antidot lattices," Phys. Rev. B **78**, 054406 (2008).

[31]D. H. Y. Tse, S. J. Steinmuller, T. Trypiniotis, D. Anderson, G. A. C. Jones, J. A. C. Bland, and C. H. W. Barnes, "Static and dynamic properties of $Ni_{80}Fe_{20}$ square antidot arrays," Phys. Rev. B **79**, 054426 (2009).

[32]B. Lenk, H. Ulrichs, F. Garbs, and M. Münzenberg, "The building blocks of magnonics," Phys. Rep. **507**, 107 (2011), and references therein.

[33]J. Ding, D. Tripathy, and A. O. Adeyeye, "Dynamic response of antidot nanostructures with alternating hole diameters," Europhys. Lett. **98**, 16004 (2012).

[34]T. Schwarze, R. Huber, G. Duerr, and D. Grundler, "Complete band gaps for magnetostatic forward volume waves in a two-dimensional magnonic crystal," Phys. Rev. B **85**, 134448 (2012).

[35]V. N. Krivoruchko and A. I. Marchenko, "Spatial confinement of ferromagnetic resonances in honeycomb antidot lattices," J. Magn. Magn. Mater. **324**, 3087 (2012).

[36]S. Tacchi, B. Botters, M. Madami, J. W. Klos, M. L. Sokolovskyy, M. Krawczyk, G. Gubbiotti, G. Carlotti, A. O. Adeyeye, S. Neusser, and D. Grundler, "Mode conversion from quantized to propagating spin waves in a rhombic antidot lattice supporting spin wave nanochannels," Phys. Rev. B **86**, 014417 (2012).

[37]J. Sklenar, V. S. Bhat, L. E. DeLong, O. Heinonen, and J. B. Ketterson, "Strongly localized magnetization modes in permalloy antidot lattices," Appl. Phys. Lett. **102**, 152412 (2013).

[38]S. Neusser, G. Duerr, R. Huber, and D. Grundler, "Spin waves in artificial crystals and metamaterials created from nanopatterned $Ni_{80}Fe_{20}$ antidot lattices," Top. Appl. Phys. **125**, 191 (2013), and references therein.

[39]G. Gubbiotti, S. Tacchi, M. Madami, G. Carlotti, R. Zivieri, F. Montoncello, F. Nizzoli, and L. Giovannini, "Spin wave band structure in two-dimensional magnonic crystals," Top. Appl. Phys. **125**, 205 (2013), and references therein.

[40]E. K. Semenova and D. V. Berkov, "Spin wave propagation through an antidot lattice and a concept of a tunable magnonic filter," J. Appl. Phys. **114**, 013905 (2013).

[41]M. Madami, S. Tacchi, G. Gubbiotti, G. Carlotti, J. Ding, A. O. Adeyeye, J. W. Klos, and M. Krawczyk, "Spin wave dispersion in Permalloy antidot array with alternating holes diameter," IEEE Trans. Magn. **49**, 3093 (2013).

[42]R. Gieniusz, V. D. Bessonov, U. Guzowska, A. I. Stognii, and A. Maziewski, "An antidot array as an edge for total non-reflection of spin waves in yttrium iron garnet films," Appl. Phys. Lett. **104**, 082412 (2014).

[43]B. Van de Wiele and F. Montoncello, "A continuous excitation approach to determine time-dependent dispersion diagrams in 2D magnonic crystals," J. Phys. D: Appl. Phys. **47**, 315002 (2014).

[44]G. Venkat, N. Kumar, and A. Prabhakar, "Micromagnetic and plane wave analysis of an antidot magnonic crystal with a ring defect," IEEE Trans. Magn. **50**, 7101104 (2014).

[45]A. Vovk, V. Golub, O. Salyuk, V. N. Krivoruchko, and A. I. Marchenko, "Evolution of the ferromagnetic resonance spectrum of a hexagonal anti-dot lattice with film thickness: Experiment and numerical simulations," J. Appl. Phys. **117**, 073903 (2015).

[46]G. Gubbiotti, F. Montoncello, S. Tacchi, M. Madami, G. Carlotti, L. Giovannini, J. Ding, and A. O. Adeyeye, "Angle-resolved spin wave band diagrams of square antidot lattices studied by Brillouin light scattering," Appl. Phys. Lett. **106**, 262406 (2015).

[47]M. Donahue and D. Porter, Interagency Report NISTIR No. 6376, NIST, Gaithersburg, MD, 1999.

[48]M. Dvornik, Y. Au, and V. V. Kruglyak, "Micromagnetic simulations in magnonics," Top. Appl. Phys. **125**, 101 (2013).

[49]W. Wang, C. Mu, B. Zhang, Q. Liu, J. Wang, and D. Xue, "Two-dimensional periodic boundary conditions for demagnetization interactions in micromagnetics," Comput. Mater. Sci. **49**, 84 (2010).

[50]C. Kittel, "On the theory of spin waves in ferromagnetic media," J. Phys. Radiat. **12**, 291 (1951).

[51]W. F. Brown, *Micromagnetics* (Interscience, New York, 1963).

[52]S. O. Demokritov, B. Hillebrands, and A. N. Slavin, "Brillouin light scattering studies of confined spin waves," Phys. Rep. **348**, 441 (2001).

[53]O. Karlqvist, "Calculation of the magnetic field in the ferromagnetic layer of a magnetic drum," Trans. R. Inst. Technol. **86**, 3 (1954).

[54]T. Schneider, A. A. Serga, T. Neumann, B. Hillebrands, and M. P. Kostylev, "Phase reciprocity of spin-wave excitation by a microstrip antenna," Phys. Rev. B **77**, 214411 (2008).

[55]O. Büttner, M. Bauer, S. O. Demokritov, B. Hillebrands, Yu. S. Kivshar, V. Grimalsky, Yu. Rapoport, and A. N. Slavin, "Linear and nonlinear diffraction of dipolar spin waves in yttrium iron garnet films observed by space- and time-resolved Brillouin light scattering," Phys. Rev. B **61**, 11576 (2000).

[56]Y. Au, M. Dvornik, O. Dmytriiev, and V. V. Kruglyak, "Nanoscale spin wave valve and phase shifter," Appl. Phys. Lett. **100**, 172408 (2012).